Kinetics and Catalysis, Vol. 45, No. 2, 2004, pp. 239–246. Translated from Kinetika i Kataliz, Vol. 45, No. 2, 2004, pp. 256–263.

CATALYTIC REACTION MECHANISMS

States of Adsorbed Hydrogen and Their Effect on the Reaction of CO Oxidation on Pd and Ta

I. I. Mikhalenko and V. D. Yagodovskii

Peoples Friendship University, Moscow, 117198 Russia

Received October 9, 2002

Abstract—Various states of hydrogen are identified on the foil and film surfaces of palladium and tantalum by photoelectric, conductivity, and thermal desorption methods. They are formed in the course of H_2 diffusion through a membrane and in the course of adsorption from the gas phase. The effect of an ethylene pyrolysis product, pyrocarbon, on the activity in CO oxidation on the palladium surface with and without H_{ads} is determined. The presence of hydrogen is found to weaken the effect of pyrocarbon. A study of hydrogen adsorption on the tantalum foil showed that hydrogen adsorption drastically declines in the presence of chemisorbed CO, but the H–Ta binding strength doubles. The fact that the sorption ability of tantalum is completely restored upon CO adsorption and partially restored upon O_2 chemisorption is achieved by thermochemical treatment in hydrogen.

INTRODUCTION

A catalytically active surface is a complex object with a variable composition and properties dependent on the chemisorbed species of substances participating in a reaction and on the modifiers introduced on purpose. The study of the states of such species and their effect on the parameters of catalytic reactions are of theoretical and practical importance.

At low concentrations, the species of a modifying adsorbate may block the active sites of a metallic catalyst and change the electron state of the free surface [1, 2], as well as its adsorption and catalytic properties [3, 4].

Palladium is a widely used and well studied catalyst for the hydrogenation and dehydrogenation of hydrocarbons, which is characterized by an ability to dissolve hydrogen in large amounts. A radically new approach to catalytic reactions with the participation of hydrogen diffusing through Pd-containing membranes has been developed in studies by Gryaznov and co-workers [5, 6].

Tantalum is also capable of sorbing hydrogen in substantial amounts. The Ta–H_2 and Pd–H_2 phase diagrams are similar [7, 8]: there is a solid solution of hydrogen in Ta and Pd and there are the hydrides PdH_2 and TaH_2. Data on the solubility of H_2 in Ta were reported in [9, 10]. The mechanism of hydrogen diffusion in Ta has been discussed in [11, 12]. Unlike palladium, the adsorption and catalytic properties of tantalum have been poorly studied. The clean surface of tantalum is chemically active, but tantalum is not very active as a catalyst because of surface passivation via the formation of oxide and carbide (oxycarbide) layers.

In this work, we studied a tantalum foil and a film. Hydrogen, the product of ethylene pyrolysis (pyrocarbon), chemisorbed carbon monoxide, and oxygen are considered as modifying agents. The effects of modifiers on the adsorption and desorption of hydrogen and on the interaction of CO with gas-phase oxygen and oxygen adsorbed on palladium are studied.

The goal of this work is to determine the charge state and the binding strengths of adsorbed and absorbed hydrogen and the effect of palladium and tantalum surface modification on their adsorption properties and their activity in the reaction of CO oxidation.

EXPERIMENTAL

The ratio of various charged states of hydrogen on the outer surface of a palladium membrane (99.9% Pd) was determined from the work function change (ϕ) in the process of hydrogen diffusion [13]. The values of ϕ were determined by the Fowler method from the dependence of the photocurrent on the frequency of incident radiation. A palladium membrane, 50 μm thick, was placed in a photoelectric cell, which was evacuated to a residual pressure of 8×10^{-7} Torr. Palladium films with continuous and island structures were obtained by the sublimation of Pd (99.9%) in a vacuum of ~10^{-7} Torr on Pyrex glass with further annealing in a vacuum at 753 K. The continuous film was ~1 μm thick and the palladium island sizes were 20–40 nm. The charge state of adsorbate and modifier species in the case of island palladium film was determined from a change in the activation energy of electric conductivity φ. The values φ were calculated from the linear form of the temperature dependence of electric resistance

$$R = AT^{-1}\exp(\varphi/kT). \quad (1)$$

The value φ linearly depends on the work function [14], and its change in the course of gas adsorption $\Delta\varphi = \varphi_0 - \varphi_{ads}$ characterizes the polarization of the adsorbed species in the same way as a change in the

0023-1584/04/4502-0239 © 2004 MAIK "Nauka / Interperiodica"

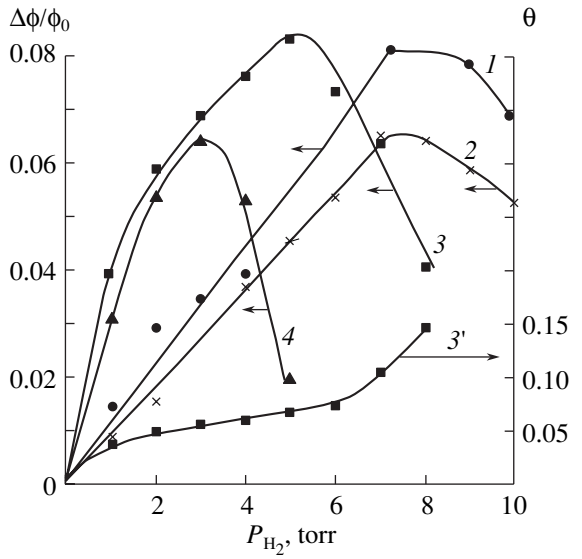

Fig. 1. Dependences of the (*1–4*) relative work function change ($\Delta\phi/\phi_0$) and (θ) the surface coverage by hydrogen at the exit side of the membrane (*3*') on the hydrogen partial pressure at the exit side of the membrane at *T*, K: (*1*) 363, (*2*) 391, (*3*, *3*') 423, and (*4*) 473.

work function $\Delta\phi = \phi_0 - \phi_{ads}$ (the subscript 0 refers to the sample before adsorption).

The kinetics of reactions CO + O_{ads} and CO + O_2 on palladium films was studied by mass spectrometry using an MX-7304 analyzer in an oil-free vacuum setup. Pyrocarbon was introduced via ethylene adsorption at 298 K with further keeping at 723 K for 1 h. Modifiers (pyrocarbon and hydrogen) and O_{ads} were dosed by the method of inleakage of gases through a capillary or an SNA-1 system of automatic injection. Oxygen was adsorbed at 398 K. Oxygen was completely absorbed during 15-min dosing. The surface coverage of palladium with O_{ads} was 0.35–0.45 ML.

The strength of hydrogen binding to palladium and tantalum was judged from the value of the activation energy of desorption E_{des} obtained from the Arrhenius plot of the rate constant of H_2 desorption in the isothermal regime under static conditions. The kinetics of O_2 (ad)sorption on Pd and H_2 (ad)sorption on Ta was studied under analogous conditions.

The tantalum foil was 20 μm thick and the apparent surface area was 120 cm^2. Before the experiments it was reduced in a flow of hydrogen at 573 K for 4 h. We obtained H_2 adsorption isotherms at 77–343 K. The kinetics of H_2 (ad)sorption were studied at 298–423 K. The kinetics of H_2 desorption were studied at 373–673 K. The effect of tantalum thermal treatment in CO and O_2 on hydrogen adsorption was also studied.

RESULTS AND DISCUSSION

Pd foil/membrane [13]. Hydrogen transfer through a membrane occurred at 363–473 K and a pressure P_{H_2} change at the entrance side of the membrane of 1 to 10 Torr. The transfer rate (*w*) depended linearly on P_{H_2}. Therefore, the limiting stage of the transfer process might be the recombinative desorption of hydrogen atoms at the exit side of the membrane [13]. The value of the work function change (ϕ) was measured from the photocurrent depending on the frequency of the incident radiation simultaneously with the hydrogen transfer rate measurements. The nature of a change in ϕ with time pointed to the fact that in the initial period negatively charged hydrogen atoms are accumulated at the exit side of the membrane (the transfer is limited by the step $H^{-\delta} + H^{-\delta} \longrightarrow H_2\uparrow$). $H^{-\delta}$ is localized in the areas with a decreased value of the work function change. Upon the settlement of the stationary regime (constant *w*), the $H^{+\delta}$ species that do not participate in the rate-limiting step are accumulated on other surface sites. Figure 1 shows a relative work function change ($\Delta\phi/\phi_0$) at the exit side of the palladium membrane in the stationary regime of diffusion at different temperatures and H_2 pressures at the entrance side of the membrane. In the absence of an adsorbate, the work function ϕ_0 is 4.3 (363, 391 K) and 4.43 eV (423, 473 K), and the work function change is $\Delta\phi = \phi_{dif} - \phi_0$, where ϕ_{dif} is the work function in hydrogen diffusion. Dependences *1–4* in Fig. 1 pass through maximums: the growth of $\Delta\phi$ means that the exit side of palladium membrane accumulates the negative charge ($H^{-\delta}$). A decrease in $\Delta\phi$ is associated with the appearance of $H^{+\delta}$. The ratio of the states of adsorbed hydrogen depends on P_{H_2}. The dependences $\Delta\phi = f(P_{H_2})$ were transformed into $\theta = f(P_{H_2})$ (where θ is the surface coverage with an adsorbate), because the work function change linearly depends on θ [15]:

$$\pm\Delta\phi = 4\pi e\mu\theta B_s, \qquad (2)$$

where B_s is the monolayer capacity, μ is the dipole momentum of an adsorbate (the value for H are taken from [16]). The plot of the dependence $\theta = f(P_{H_2})$ is S-shaped (Fig. 1, curve *3*'), which reflects the formation of differently charged hydrogen atoms at the exit side of the membrane, their fractions are 4–9% for $H^{+\delta}$ and 5–6% for $H^{-\delta}$.

For instance, at T = 391 K, $\theta = \dfrac{\Delta\phi}{4\pi e\mu B_s} = \dfrac{0.3\times1.6\times10^{-12}}{4\times3.14\times4.8\times10^{-10}\times1\times10^{-18}\times0.9\times10^{15}} = 0.088.$

The value B_s (cm^{-2}) is calculated taking into account the membrane roughness coefficient (K_{rough} = 2.1) determined from argon adsorption. A possible mechanism of

hydrogen transfer that agrees with the above estimates can be as follows:

$$H_2 + 2s \longleftrightarrow 2H\text{-}s, \quad \text{(I)}$$

$$H\text{–}s + v \longleftrightarrow H\text{–}v + s, \quad \text{(II)}$$

$$H\text{–}v + s^* \longleftrightarrow H^{-\delta}\text{–}s^* + v, \quad \text{(III)}$$

$$2H^{-\delta}\text{–}s^* \longrightarrow H_2 + 2s^*, \quad \text{(IV)}$$

where $[H^{-\delta}\text{–}s^*] = \theta$ is the surface coverage by hydrogen atoms at the exit side of the membrane, v are the sites for hydrogen localization in the bulk, and s are the sites for adsorption at the exit side of the membrane.

If we assume that the equilibrium coverage of the entrance side of the membrane by hydrogen atoms is described by the Langmuir equation for dissociative adsorption and step (IV) is assumed to be rate-limiting, then we can derive the following equation

$$\theta = \frac{A\sqrt{P_{H_2}}}{B + A\sqrt{P_{H_2}}}, \quad (3)$$

in which A and B are expressed in terms of the rate constants of steps (I)–(IV) and the adsorption coefficient of the Langmuir equation. Equation (3) describes well the dependence $\theta = f(P_{H_2})$.

It was found that the products of ethylene and acetylene chemisorption at the exit side of the membrane led to a drastic decrease in the rate of hydrogen transfer through the membrane. This fact supports the choice of the rate-limiting step.

Pd films. The kinetics of hydrogen desorption from the continuous Pd film suggests the existence of three states of adsorbed hydrogen with activation energies of desorption of 33 ± 6 (state 1), 84 ± 8 (state 2) and 117 ± 8 kJ/mol (state 3). These are independent of the pressure and temperature of the preliminary H_2 desorption. In hydrogen desorption from the island film of Pd two states of hydrogen were identified with activation energies of desorption E_{des} = 21–33 kJ/mol (state 1) and E_{des} = 84 ± 8 kJ/mol (state 2). The strongly bound state (state 3) has not been found. State 1 corresponds to hydrogen dissolved in the near-surface layer of the metal. With an increase in the initial pressure of H_2 and a decrease in the temperature of adsorption, the amount of state 1 increases.

The adsorption of hydrogen by palladium films is accompanied by an increase in the activation energy of electric conductivity φ. The values $\Delta\varphi = \varphi_0 - \varphi_{ads}$ are negative. Therefore, the predominant states of hydrogen adsorption is the $H^{-\delta}$ atom formed on the surface sites with low work function and/or atoms localized in the near surface layer of palladium $H^{+\delta}_{sub}$ (these states are indistinguishable from Δφ).

In hydrogen desorption, the change φ is reversed. Figure 2 shows the dependence $\Delta\varphi = \varphi_0 - \varphi_{des}$ (adsorption temperature, 363 K). It is seen that, in the hydrogen

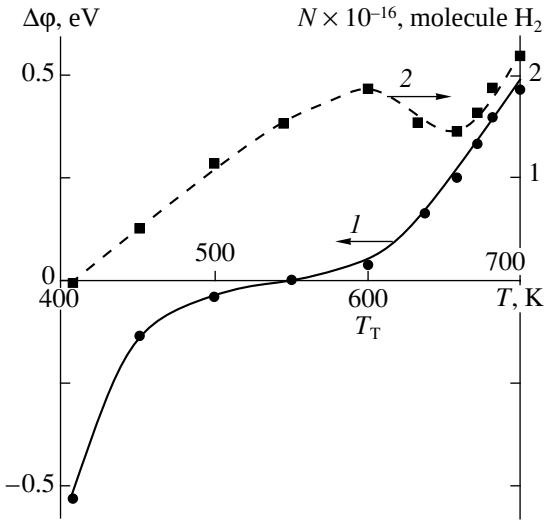

Fig. 2. Temperature dependences of the activation energy of electric conductivity of the palladium film in (*1*) H_2 desorption and (*2*) the amount of desorbed hydrogen.

desorption temperature range 393–553 K, the values φ are negative meaning that the $H^{-\delta}(H^{+\delta}_{sub})$ states dominate. With an increase in the temperature, their concentration decreases and the fraction of $H^{+\delta}$ species increases, as is evident from an increase in $\varphi_{дес}$. The sign of palladium surface polarization changes at 500–600 K. At temperatures of 393–603 K, the most weakly bound hydrogen states $H^{-\delta}$ and/or $H^{+\delta}_{sub}$ with E_{des} = 21–33 kJ/mol are desorbed. At temperatures above 623 K the state $H^{-\delta}$ (2) with E_{des} = 84 kJ/mol is desorbed. The formation of two states of adsorbed hydrogen atoms with negative polarization can be explained by metal surface nonuniformity. At 500–600 K, the effective charge of the surface is close to zero. A dashed line in Fig. 2 shows an increase in the amount of desorbed H_2 molecules, but hydrogen readsorbs at 600–630 K. Note that this is in the range of the Tamman temperature $T_T = 0.33T_{melt}$, above which new sites can be formed due to the surface mobility of the palladium atoms. At T > 630 K hydrogen state *2* ($H^{-\delta}$) begins to desorb.

Consider the effect of palladium modification by the products of ethylene pyrolysis and adsorbed hydrogen on the charge of palladium particle surface. This is important for considering the catalytic oxidation reactions in the presence of H_2. Thus, when hydrogen is added to a CH_4–O_2 mixture, an increase in the yield of valuable products (methanol and formaldehyde) is observed because methane activation becomes more favorable [17, 18]. The detailed mechanism for H_2 effect remains unclear.

In this work we consider the effect of palladium modification by pyrocarbon (PC) and hydrogen using model processes: oxygen chemisorption and the reactions $CO + O_{ads}$ and $CO + O_2$. The kinetics of these pro-

Table 1. The change in the activation energy of electric conductivity of the palladium film in the modification by (**B**) pyrocarbon and (**C**) hydrogen

T, K		423	473	523	550	573
Δφ, eV	**B**	−0.10	−0.13	−0.13	−0.12	−0.11
	C	0.15	0.18	0	−0.20	−0.15

Note: $\Delta\varphi = \varphi_0 - \varphi_{mod}$.

Table 2. Effect of palladium film modification on the kinetics of O_2 chemisorption

Pd state	**A**	**B**	**C**(**C'**)	**D**
k_{O_2}, s^{-1} (473 K)	0.256	0.015	0.110 (0.07)	0.040
E_{O_2}, kJ/mol	5.9 ± 0.8	19.2 ± 1.8	10.5 ± 1.2 (12 ± 1)	14.6 ± 1.2

cesses was studied for four states of the palladium film surface: initial (state **A**), after addition of pyrocarbon with θ_{PC} = 0.05 (state **B**), after combined addition of pyrocarbon and hydrogen with θ_{PC} = 0.05 and θ_H = 0.75 (**C**, **C'**), and after addition of hydrogen with θ_H = 0.75 (**D**). The value θ_H is considered conditional because of possible hydrogen dissolution in the near-surface layer of palladium. States **C** and **C'** differ in the order of modifier addition: PC + H_2 (**C**) and H_2 + PC (**C'**). The products of the interaction of modifiers with oxygen and CO have not been found (H_2O was also absent).

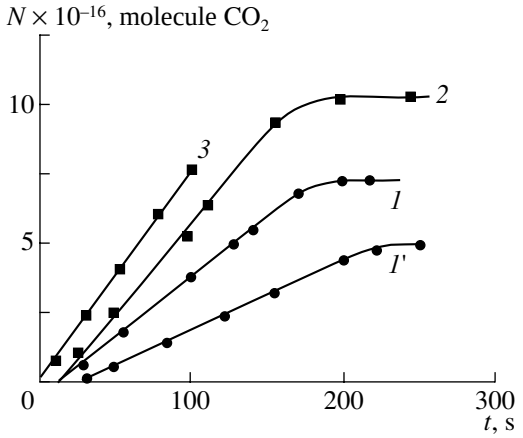

Fig. 3. Time dependences of the amount of CO_2 formed in the reaction of CO with adsorbed oxygen on the palladium film at (*1–3*) 303 and (*1'*) 586 K for three states of the surface: (*1*, *1'*) initial, (*2*) in the presence of pyrocarbon with the coverage $\theta_{pyrocarbon}$ = 0.05, and (*3*) in the presence of hydrogen with θ = 0.75.

Upon modification, the charges of the modifier species were determined from the value φ of the film for temperatures at which O_2 adsorption and the reaction O_{ads} + CO were studied. The values presented in Table 1 $\Delta\varphi = \varphi_0 - \varphi_{mod}$ suggest that the products of ethylene pyrolysis have a negative polarization ($C^{-\delta}$ and $CH^{-\delta}$): after modification, φ increases (Δφ < 0).

At low temperatures in the presence of hydrogen, the charge of the surface modified by pyrocarbon changes to the opposite (Δφ > 0). This can be explained by the presence of the competing species $H^{+\delta}$. However, with an increase in the temperature the sign of hydrogen polarization changes to the opposite $H^{+\delta} \longrightarrow H^{-\delta}$, which is favored by a decrease in the work function. At $T > 550$ K the modified surface is negatively charged (Δφ < 0).

Oxygen adsorption and reactions CO + O_{ads} and CO + O_2. The rate of oxygen adsorption w_{O_2} was determined at 293–573 K. The adsorption constants k_{O_2} calculated from equation $w_{O_2} = k_{O_2} P$ increase with an increase in the temperature pointing to oxygen chemisorption. The surface coverage with oxygen was at most 5%. Table 2 shows the values of k_{O_2} for 473 K and the values of the activation energy of oxygen chemisorption.

The products of pyrolysis and hydrogen drastically retard oxygen chemisorption. The value of k_{O_2} decreases in the presence of pyrocarbon to a greater extent, although its concentration is 15 times lower than the concentration of hydrogen. However, when they are introduced together, the effects of these two components are not additive. The activation energy of oxygen chemisorption triples upon the introduction of pyrocarbon onto the surface, but the modifying effect of pyrocarbon introduced together with H_{ads} is lower. This is probably due to the formation of adsorbed $H^{+\delta}$ atoms in the presence of $C^{-\delta}$ and $CH^{-\delta}$. These atoms compensate for the negative charge of the palladium surface with pyrocarbon (Table 1) and favor oxygen dissociation.

The interaction of CO with adsorbed oxygen substantially depends on the presence of surface admixtures. Figure 3 compares the kinetics of the reaction CO + O_{chem} at 303 K for the initial palladium surface and the surface modified by pyrocarbon and hydrogen at the same amounts of modifiers as in the case of oxygen chemisorption. We found that for all states, the reaction rate decreases with an increase in the temperature (see curves *1* and *1'*). This is due to the redistribution of oxygen between the surface and near-surface layers of the metal. The negative temperature coefficient of the CO oxidation reaction agrees with the literature data [19]. In our earlier work [4], we found that pyrocarbon on the surface of dispersed nickel also inhibits the reaction CO + O_{ads} at a surface coverage of $\theta_{pyrocarbon}$ = 0.1–1.6, but this happens at a reaction temperature below 423 K. At $\theta_{pyrocarbon} < 0.2$, the products

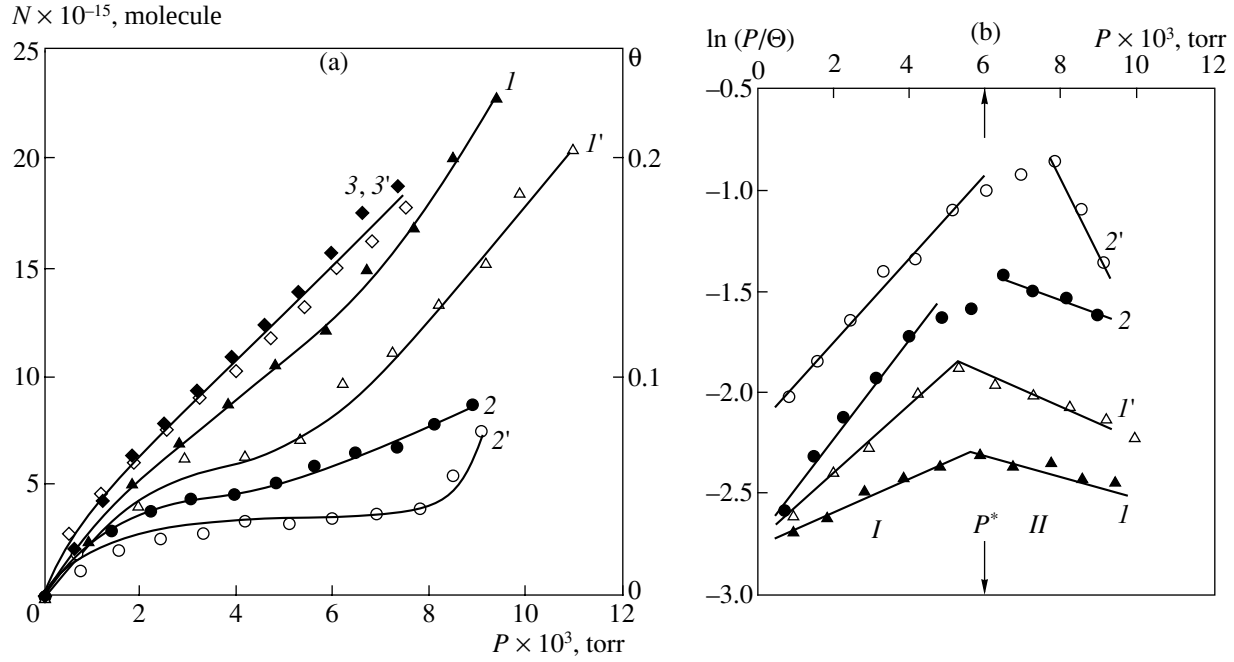

Fig. 4. (a) H_2 adsorption isotherms for the tantalum foil at (*1*, *1*') 77, (*2*, *2*') 273, and (*3*, *3*') 298 K in two consecutive runs: (*1*'–*3*') first and (*1*–*3*) second; (b) their description in the linear coordinates of Eq. (6).

of ethylene pyrolysis promote CO oxidation. The introduction of hydrogen onto the palladium surface also leads to an increase in the rate of CO_2 formation. The promoting effect of H_{ads} is due to a decrease in the strength of O_{ads} binding to palladium because of the $H^{+\delta}$ adsorption on the sites with a high binding strength and because of the presence of $H^{-\delta}$ atoms that decrease the adsorption potential of the free portions of the metal surface [2].

The kinetics of the reaction CO + O_2 was studied in the temperature range 312–623 K at O_2 and CO pressures of 0.04 and 0.015 Torr, respectively, on the initial film of Pd and after pyrocarbon introduction in an amount of 0.1 ML.

In the case of the first sample, the rate of the reaction CO + O_2 passed through a maximum at 443 K. In the case of the second sample, the rate continuously increased with the temperature [20]. Analogous dependences were obtained for clean palladium in [21, 22] and a four-step reaction mechanism was proposed:

$$CO + s^* \longleftrightarrow CO_{ads}, \quad \text{(I')}$$

$$O_2 + s^* \longleftrightarrow 2O_{ads}, \quad \text{(II')}$$

$$O_{ads} + CO \longrightarrow CO_2, \quad \text{(III')}$$

$$O_{ads} + CO_{ads} \longrightarrow CO_2. \quad \text{(IV')}$$

According to this scheme, the overall rate of the reaction is

$$W = [O_{ads}](k_3 P_{CO} + k_4[CO_{ads}]), \quad (4)$$

where k_3 and k_4 are the rate constants of steps (III) and (IV).

It was shown in [22] that the rate constants of adsorption steps k_1 and k_2 are approximately equal. Therefore,

$$w \approx 2\frac{k_2 k_{-1} P_{O_2}}{k_1 P_{CO}}. \quad (5)$$

Under these conditions, the activation energy of the reaction is approximately determined by the heat of CO adsorption. However, above 450 K the average time of CO molecule residence on the surface decreases to 10^{-2} s and CO desorption begins, which explains the decrease in the reaction rate. On the modified surface, the reaction rate in the range 450–500 K was lower than on the initial surface, whereas at T > 550 K it was higher. At T > 550 K, the value φ in the presence of pyrocarbon increases by 30% and, according to [2], the heat of CO increases and favors an increase in the amount of CO_{ads}.

Thus, the modifying action of small amounts of pyrocarbon plays an important role, and this can be interpreted as a change in the collective electron properties of the surface. In the presence of hydrogen, the inhibition by carbon-containing species is smoothed.

Ta foil. The isotherms of hydrogen adsorption on Ta are shown in Fig. 4. It can be seen that they resemble curve *3*' in Fig. 1. The complex shape of the isotherms can be explained by the fact that the dissolution of hydrogen in the near-surface layer of tantalum (the H_{sub} state) initiates further H_2 adsorption: the state of surface sites changes in the presence of H_{sub}, and this is reflected in the induced adsorption [23, 24]. This is also

Table 3. Induced hydrogen adsorption on the tantalum foil in two consecutive runs*

T, K	ΔN, %		Parameters of the Langmuir equation**		$B_{12}^{(2)}/B_{12}^{(1)}$		ΔQ_o, %	
	I	*II*	ΔN_m, %	$K^{(2)}/K^{(1)}$	*I*	*II*	*I*	*II*
77	50	40	250	0.2	0.4	0.7	0	28
273	30	44	44	1.24	1.3	0.1	29	–130

*First and second runs are marked with superscripts (1) and (2). *I* and *II* are the intervals of pressure designated in Fig. 4b.
**Calculated for pressure interval *I*.

supported by an increase in the adsorption in two successive experiments at the same temperature, e.g., at 77 and 273 K (Fig. 4), between which the gas phase was only evacuated for 10 min. The isotherms of the first and second runs are different and the value of induced adsorption expressed as an increase in the amount of the adsorbate $\Delta N = (N^{(2)} - N^{(1)})/N^{(1)}$ is 30–50% (Table 3).

The initial portions of H_2 adsorption isotherms (before a plateau or an inflection point P^* (Fig. 4)) can be analyzed in the framework of the model Langmuir equation. An increase in the adsorption at 77 K by 50% corresponds to an increase in the effective monolayer capacity N_m by a factor of 2.5 in the second run and a decrease in the adsorption coefficient $K^{(2)}/K^{(1)} = 0.2$ by a factor of 5 (Table 3). At 273 K, the induced adsorption is associated with an increase in N_m and K.

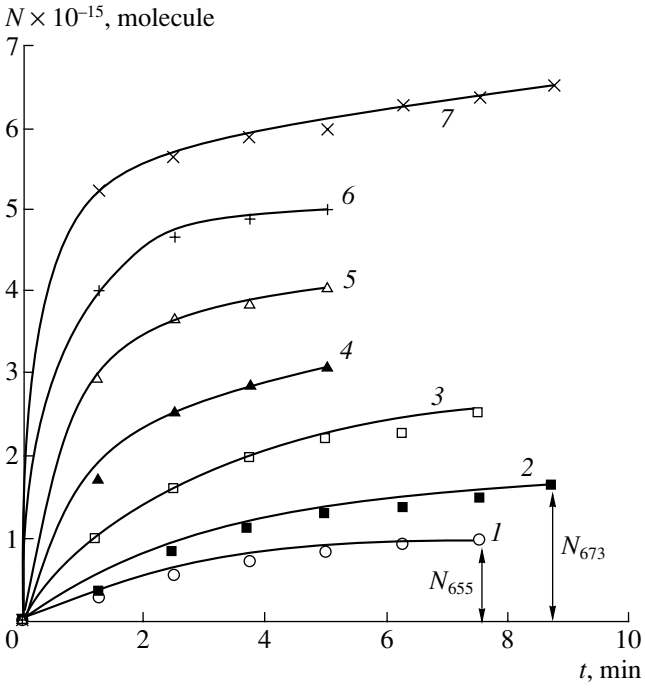

Fig. 5. Kinetics of hydrogen thermal desorption from tantalum foil (the temperature of H_2 adsorption, 473 K) at various temperatures, K: (*1*) 655, (*2*) 673, (*3*) 693, (*4*) 713, (*5*) 733, (*6*) 751, and (*7*) 773.

The phenomenon of induced adsorption, which is explained by the effect of dissolved hydrogen H_{sub} can be analyzed using the equation of the adsorption isotherm (4) [23, 24] that takes into account the interactions of metal electrons with an adsorbate via the virial coefficient B_{12}:

$$\theta = AP\exp\left[\frac{Q_0}{RT} - \left(\frac{B_{12}}{B_{11}}\right)\frac{B_0 CP}{RT}\right], \qquad (6)$$

where Q_0 is the initial heat of adsorption; the sign of B_{12} is determined by the ratio between the Coulomb and polarization terms in the expression for the potential of the pairwise interaction; B_{11} is a constant ($B_{11} > 0$) that takes into account the interaction of metal electrons between each other; B_0 is the Henry constant, and A and C are some constants.

S-shaped adsorption isotherms in the $\ln(P/\theta)$–P coordinates (Fig. 4b) have two linear segments corresponding to the convex (*I*) and concave (*II*) parts of (Fig. 4a) from which B_{12} and the initial heat of adsorption Q_0 are found. The ratios $B_{12}^{(2)}/B_{12}^{(1)}$ and changes in the initial adsorption heat $\Delta Q_0 = (Q_0^{(2)} - Q_0^{(1)})/Q_0^{(1)}$ in percents are shown in Table 3. In the range of low pressures ($P < P^*$) $B_{12} > 0$ and in the case of $P > P^*$ the sign of B_{12} changes ($B_{12} < 0$). At $T = 77$ K and low hydrogen pressures, the induced adsorption is due to a decrease in B_{12} by a factor of 3 without changes in the heat of adsorption. At 273 K adsorption increases due to an increase in both parameters. In the region of high pressures, the value of Q_0 decreases by a factor of ~2, and B_{12} decreases by a factor of 10.

Thus, changes in the shape of the adsorption isotherm with an increase in the H_2 pressure can be explained by a change in the sign of B_{12} and by a decrease in the initial heat of adsorption due to the effect of absorbed hydrogen. The nature of this effect depends on the adsorption temperature and the H_2 pressure.

Table 4. H_2 desorption from the tantalum foil before and after CO chemisorption [25]

Parameters	Temperature of H_2 adsorption, K		
	473*	523*	523
Interval of desorption temperatures, K	673–773	613–723	673–773
$N_{max} \times 10^{-15}$, molecule	40	185	56
$w_{713\,K} \times 10^{-17}$, molecule/min	23	690	15
$E_{des,\,1}$, kJ/mol ($\ln k_0$)	**173**(65)	**146**(64)	**280**(82)
$E_{des,\,2}$, kJ/mol	76	60	115
$E_{des,\,1} - E_{des,\,2}$, kJ/mol	96	86	165

*Before CO chemisorption.
** After CO chemisorption.

The binding strength of hydrogen strongly adsorbed on the tantalum surface was determined by the thermal desorption method. Figure 5 shows a sample of the dependence of the amount of desorbed hydrogen on time at a constant temperature. These data were used to calculate the initial rates of desorption $w_{des,\,0}$ and the rate constants assuming second-order desorption: $k_{des} = w_{des,\,0}/\theta^2$. The dependences of $\ln k_{des}$ on T^{-1} were used to calculate the activation energies of desorption $E_{des,\,1}$ with an accuracy of ±2–6 kJ/mol. The upper limit of desorbed hydrogen ΔN_{des} and the dependences $\ln \Delta N_{des} = f(T^{-1})$ were used to calculate the activation energies of desorption $E_{des,\,2}$. The values of $E_{des,\,2}$ characterize the desorption process at the final stage (after the removal of hydrogen atoms from the surface), which is limited by hydrogen atom transfer from the near-surface layer onto the surface $H_{sub} \longrightarrow H_s$. The activation energy of the $H_{sub} \longrightarrow H_s$ transfer can be estimated as the difference $E^* = E_{1,\,des} - E_{2,\,des}$. The values $E_{1,\,des}$ and $E_{2,\,des}$ and the temperature intervals in which they were determined, as well as the maximal amount of desorbed H_2 (N_{max}), are presented in Table 4. For the initial surface of the tantalum foil, preliminary H_2 adsorption was carried out at 473 and 523 K. Then the temperature was decreased to ambient, and the foil was allowed to stay in H_2 for 12 h. After evacuating the gas phase, the kinetics of desorption were studied with temperature ramping.

Data presented in Table 4 suggest that, with an increase in the adsorption temperature from 473 to 523 K, the amount of strongly adsorbed hydrogen N_{max} increases by a factor of 4. Desorption begins at lower temperatures. The desorption rates and the rate constants of desorption increase dozens of times (cf., for instance, $w_{713\,K}$). This is due to a decrease in the activation energy of desorption $E_{1,des}$. After CO chemisorption, new sites are formed: the H_s–Ta(CO) strength doubles (280 vs. 146 kJ/mol). The strength of absorbed hydrogen H_{sub} binding also increases (from 86 to 165 kJ/mol).

The ability of a tantalum foil to absorb hydrogen largely depends on the chemisorbed species. Upon CO chemisorption, the rate constants of H_2 (ad)sorption decrease several times. A decrease in H_2 sorption is observed upon O_2 chemisorption as well. The rate constants of H_2 adsorption were calculated using the equation $k_{ads} = w_{ads}/P_0(H_2)$, where w_{ads} is the rate of H_2 adsorption determined from the linear plots of adsorbed H_2 versus time. The rate of H_2 adsorption linearly increased with an increase in the initial pressure – $P_0(H_2)$.

Table 5 shows the effect of tantalum treatment in various gases on the kinetics of H_2 sorption at 423–543 K. To restore the sorption properties of tantalum, simple (*1–4* and *7*) and consecutive/combined thermal treatments (*5* and *6*) were applied in H_2.

The products of CO and O_{chem} chemisorption deactivate the tantalum surface. Upon CO chemisorption, the sorption ability can be partially restored by simple treatment in H_2 (compare *1* with *3* and *4*). Analogous regeneration in H_2 upon O_2 chemisorption is less effective: the rate constant of hydrogen adsorption triples, but the value of k_{ads} is 4 times lower than the initial one. Tantalum deactivation upon thermal treatment with O_2 is irreversible and can be associated with the formation of an oxide layer.

Thus, changes in the adsorption and catalytic characteristics of palladium under the action of small amounts of modifiers (pyrocarbon and H_{ads}) are due to a change in the electron state of the surface (a collective effect). In the case of tantalum, the effect of CO and oxygen chemisorption on H_2 adsorption is due to the

Table 5. Parameters of H_2 sorption after thermal treatments of the tantalum foil

Parameter	Treatment						
	1 (H_2O)	**2** (CO)	**3** (H_2)	**4** (H_2)	**5** (O_2 + CO + H_2)	**6** (H_2 + CO)	**7** (H_2)
$k_{ads} \times 10^{-17}$, min^{-1} (463 K)	2.4	0.6	1.8	1.9	0.2	0.5	0.6
E_{ads}, kJ/mol	28.5	33	28	20	36	28	24

formation of strongly chemisorbed layers formed from CO and O_2.

REFERENCES

1. Temkin, M.I., *Zh. Fiz. Khim.*, 1941, vol. 44, no. 2, p. 495.
2. Yagodovskii, V.D. and Rei, S.K., *Zh. Fiz. Khim.*, 1982, vol. 56, no. 9, p. 2360.
3. Lebedev, N.I., Mikhalenko, I.I., and Yagodovskii, V.D., *Kinet. Katal.*, 1999, vol. 40, no. 4, p. 590 [*Kinet. Catal.* (Engl. Transl.), vol. 40, no. 4, p. 532].
4. Mikhalenko, I.I., Katre, A., and Yagodovskii, V.D., *Kinet. Katal.*, 2000, vol. 41, no. 2, p. 233 [*Kinet. Catal.* (Engl. Transl.), 2000, vol. 41, no. 2, p. 211].
5. Gryaznov, V.M., *Kinet. Katal.*, 1971, vol. 12, no. 3, p. 640.
6. Orekhova, N.V., Basov, N.L., Ermilova, M.M., and Gryaznov, V.M., *Zh. Fiz. Khim.*, 1994, vol. 68, p. 2139.
7. Kobler, U. and Welter, I.M., *J. Less-Common Met.*, 1982, vol. 8, p. 225.
8. *Metals Reference Book*, Smithells, K.L., Ed., Boston: Butterworths, 1976.
9. Ivashina, Yu.K., Nemchenko, V.F., and Ivashchina, T.A., *Zh. Fiz. Khim.*, 1980, vol. 54, no. 11, p. 2827.
10. Katlinskii, V.M. and Egorova, V.M., *Zh. Fiz. Khim.*, 1980, vol. 54, no. 3, p. 757.
11. Verbetskii, V.N. and Sirotkina, R.A., *Izv. Akad. Nauk SSSR, Ser. Khim.*, 1990, vol. 4, p. 195.
12. Weisser, M. and Kalbitzer, S., *Z. Phys. Chem.*, 1985, vol. 143, p. 183.
13. Zubarev, Yu.A., Mikhalenko, I.I., and Yagodovskii, V.D., *Kinet. Katal.*, 1983, vol. 24, no. 5, p. 1194.
14. Yagodovskii, V.D., *Zh. Fiz. Khim.*, 1974, vol. 48, no. 5, p. 1093.
15. Kaminsky, M., *Atomic and Ionic Impact Phenomena on Metal Surfaces*, Berlin: Springer, 1965.
16. *Solid State Surface Science*, Green, M., Ed. New York: Marcel-Dekker, 1969, vol. 1.
17. Otsuka, K. and Yamanaka, I., and Wang, Y., *Stud. Surf. Sci. Catal.*, 1998, vol. 119, p. 15.
18. Min, J.-S., Ishipe, H., Misono, M., and Mizuno, N., *J. Catal.*, 2001, vol. 198, p. 116.
19. Boreskov, G.K., *Geterogennyi kataliz* (Heterogeneous Catalysis), Moscow: Nauka, 1986.
20. Sarychev, V.I., *Cand. Sci. (Chem.) Dissertation*, Moscow: Moscow People's Friendship Univ., 1988, p. 173.
21. *Catalysis*, Ertl, G. and Koch, J., Eds., Amsterdam: Hightower, 1973, vol. 2, p. 969.
22. Engel, C. and Ertl, G., *J. Chem. Phys.*, 1978, vol. 63, no. 3, p. 1267.
23. Bratchikova, I.G., Mikhalenko, I.I., Sapata, O.-L., and Yagodovskii, V.D., *Zh. Fiz. Khim.*, 2001, vol. 75, no. 5, p. 914 [*Russ. J. Phys. Chem.* (Engl. Transl.), vol. 75, no. 5, p. 818].
24. Mikhalenko, I.I. and Yagodovskii, V.D., *Zh. Fiz. Khim.*, 2002, vol. 76, no. 4, p. 600 [*Russ. J. Phys. Chem.* (Engl. Transl.), vol. 76, no. 4, p. 516].
25. Bratchikova, I.G. and Mikhalenko, I.I., *Zh. Fiz. Khim.*, 2001, vol. 75, no. 5, p. 717.